Proceedings of the 9th World Congress on Civil, Structural, and Environmental Engineering (CSEE 2024)
London, United Kingdom – April 14-16, 2024
Paper No. ICGRE 126
DOI: 10.11159/icgre24.126

Stability Analysis of Surface and Subsurface Geological Hazards Using Numerical Approach in Hydropower Project of India- a Case Study

Mainak Ghosh Roy[1], Nirmal Singh[2], Sajan Moideen[2]

[1]NHPC Ltd.
Parbati Hydroelectric Project-II, Nagwain, Himachal Pradesh, India
mainakghosh@nhpc.nic.in; nirmalsingh@nhpc.nic.in

[2]NHPC Ltd.
Parbati Hydroelectric Project-II, Nagwain, Himachal Pradesh, India
sajan@nhpc.nic.in

Abstract **–**The paper reviews major geological problems encountered during construction of a mega hydropower project in the Lesser Himalayan region of Himachal Pradesh, India. Major hindrances encountered during construction of the project were backslope failure during construction of surface powerhouse in metavolcanics with slumped rockmass and rock bursting during tunnelling in hard and brittle quartzite. Two different modes of failures occurred during excavation of 180m long backslope of surface Powehouse-circular failure along highly weathered slumped rockmass and planar failure along crushed rock filled valley dipping joints. Stability assessment of powerhouse backslope was carried out through Finite element based software and Limit equilibrium based software for analysis of planar failure in jointed rockmass and determine critical slip circle of failure and Factor of Safety of the slope through strength reduction technique. Optimum support analysis for stabilization of cutslope was carried out through numerical simulation. Deformation meshes, accumulated principal strain and total displacement are the other parameters obtained from the results computed and analysed using FEM. The paper also back analyzes magnitude of in-situ stresses in rock bursting zones encountered during tunnelling using finite element based software to determine role of depth of overburden and field stress ratio in causing rock bursting. The result indicates that yielding zones increase with depth of overburden and decrease in field stress ratios.

Keywords**:** Slope Stability, Numerical Analysis, Factor of Safety, In-situ Stresses, Rock Bursting

1. Introduction

Being youngest of the mountain chains, Himalayas arguably pose the most challenging ground conditions although there is a huge potential of surface and underground constructions in the Himalayan region for hydropower and infrastructure development. The common geological hazards often encountered in Himalaya are thrust/shear zones, stress induced deformations like rock bursting and squeezing, ingress of groundwater, variety of slope failure processes which includes various kinds of rockfalls like planar, wedge, toppling and circular failure governed by the pattern of rock discontinuities. The paper reviews two major geological hindrances viz. 180m high backslope failure of powerhouse and rock bursting during excavation of 31.5km long headrace tunnel which were experienced in Parbati hydroelectric project-II, a 800MW capacity project in Lesser Himalayan region of India, presently under construction by NHPC Ltd.

2. General Description of Project

Parbati hydroelectric project-II is a run of river scheme located in Himachal Pradesh, India on the river Parbati, a tributary of Beas river. Major part of the project area falls within a tectonic window in close proximity to Jutogh thrust which is a part of Main Central Thrust. Project mainly comprises construction of 85m high Concrete Gravity Dam, 31.5km long, 6.0m diameter Head Race Tunnel, two 1.5km long inclined pressure shafts of 3.5m diameter and a surface power house (123m x 47m x 44m). The power house utilizes a gross head of 862m and will have installed capacity of 800 MW. Layout plan of the project is shown in Fig. 1(a).

3. Major Geological Hazards Encountered During Surface Excavation

3.1. Backslope Failure of Surface Powerhouse

The failures of slopes in Himalaya are common particularly along the zones lying in close proximity of two major

(a) (b)

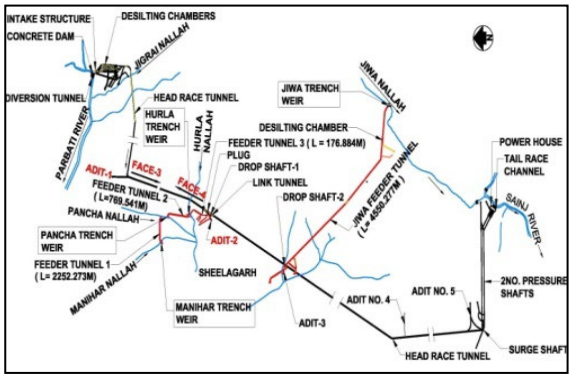

Fig. 1: (a) Layout plan of Parbati hydroelectric project-II (b) View of surface powerhouse of Parbati hydroelectric project-II

tectonic units i.e. Main Boundary Thrust (MBT) and Main Central Thrust (MCT) where the neo-tectonic activities along the zones of major thrusts cause a high frequency of slope failure (Valdiya and Bartarya, 1989). In the present study, causative factors of the backslope failure in Parbati hydroelectric project-II are discussed. Further, numerical simulation is carried out with both Finite element and Limit equilibrium method to evaluate the failure mechanisms and factor of safety of the powerhouse backslope.

3.2. Geology of the Powerhouse Area

The surface powerhouse (Fig.1b) was constructed on a 40m wide multistage riverine terrace. The back slope of the powerhouse rises steeply (~45º) upto a height of 180m rising from El±1330M to EL±1510M beyond which a break in slope has resulted into relatively gentler slope of 25-30º upto the surge shaft ridge. During excavation, powerhouse slope was covered with thick slope wash material whereas, the rock was exposed as steep escarpment around the surge shaft area. The bedrock in the powerhouse backslope area comprises of low grade metamorphic rocks of metabasics and chlorite schist. The bedrock is overlain by slope wash material and slumped rock mass at few places. The rock is dissected by one prominent foliation joint set (070º/50º) and one valley dipping joint set (150º/60º).

During investigation stage, the powerhouse area was thoroughly investigated by exploratory drilling, drifts and geophysical surveys. Two level drifts were excavated at El ±1350M and ±1346M respectively as shown in Fig. 2(a). Weak geological features such as sheared/crushed zone, rock flour/crushed rock filling along the joint plane, opening of upto 50mm along joint plane were observed in the drift. About 25-50% rockmass encountered in the drift belonged to poor to very poor category as per RMR classification. The presence of open joint planes (2mm to 100mm) in the drift indicates partial slumping of rockmasses upto an observed depth of 15 to 20m (Bhatnagar & Das, 2013).

3.3. Design and Methodology of Powerhouse Excavation

From upstream to downstream portion, the entire powerhouse slope was divided in -6 to + 30 RD segment. The straight portion in the upstream from RD -6m to RD+24m was cut sub-perpendicular to the foliation whereas the cut faces in the downstream curved portion from RD+24m to RD+30m are sub parallel to the foliation planes.

The excavation of powerhouse backslope was designed in steps of 15m with berm width of 4m as shown in Fig. 2 (b). The excavation was initially proposed upto EL.1417M with cut line at El. 1423M with recommended support measures of 6 to 9m long, 25-36 mm dia rock anchors along with wire mesh and shotcrete. During preliminary stage of rock cutting, no sound rock mass were encountered along the cut line in the upstream portion from RD -5m to +4m due to which, the rock cutting started from higher elevation at around El 1450M. However, due to non-availability of sound and firm rock even upto El 1450M, loose boulders were removed and remaining surface comprising of bedrock overlain by slumped rockmass was treated with wire mesh and shotcrete along with rock anchors.

(a)

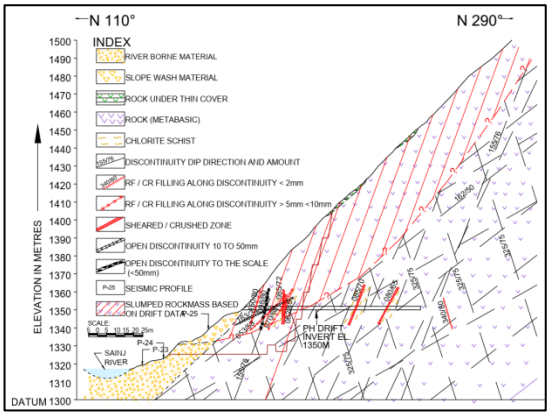

Fig. 2: (a) Geological section of Powerhouse backslope

(b)

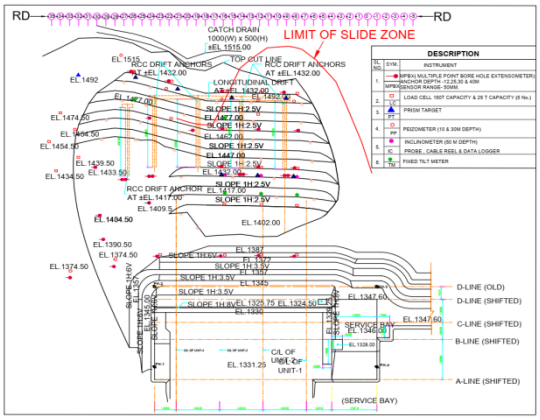

Fig. 2: (b) Powerhouse excavation and instrumentation plan

3.4. Slide in Powerhouse Area between RD -7m to +9m

During excavation of powerhouse backslope in the service bay area between RD-7m and RD+9m, 1-50mm wide cracks started to develop at the beginning. Later on these cracks resulted into slide starting from El ±1440M to ±1368M. This slide later on extended upto El ±1480M. Prior to failure, heavy rainfall further triggered rotational movement of rockmass along the weak plane (Fig. 3a). Slumped rockmass alongwith valley dipping joints with low shear strength vis-à-vis heavy precipitation culminated into slip circle failure and caused major slide in the service bay area (Fig. 3b). To monitor the behaviour of rockmass, 6-15m long Single/Multi-point borehole extensometers were installed in the cut slopes. A major jump in the instruments readings and increase in width of the cracks upto 10cm were observed before failure.

Restoration of the slope was carried out by slope dressing, wire meshing, installation of 6m and 9m long rock anchors, 25mm dia and 6m long soil nail and 150mm thick shotcrete in two layers. Drainage/pressure relief holes of length 3-4 m were also provided. The estimated amount of slided muck was around 30,000m^3 to 35,000 m^3.

(a)

(b)

Fig. 3:a,b. View of slide in the u/s of powerhouse cut slope between RD -7m and +9m starting from El±1440M to El±1368M

3.5. Numerical Modelling for Stability Analysis of Powerhouse Backslope

To carry out slope stability analysis, a two dimensional finite element model of the unsupported slope was created using Finite Element model (FEM) Plaxis 2D. An unsupported excavation of the cut slope will cause the instability of the rock slope. The geometry of the natural sloping ground wherein the cut slope was excavated is considered to be metabasics bedrock with slumped rockmass upto a depth of 20m alongwith open joints extending upto the entire height of the slope as shown in Fig. 4. A plane strain model is used with uniform cross sections. The laboratory rock mechanic properties of metabasics, slumped rockmass and crushed rockfill along open joints are shown in Table 1.

To solve any geotechnical problem using Plaxis 2D, the components of a problem certify three conditions i.e. generation of mesh, constitutive behaviour and material properties and boundary conditions (Singh et al, 2005). In this project, the metabasic rock mass is modelled using the Hoek-Brown constitutive model and slumped rockmass is modelled using Mohr-Coulomb elasto-plastic model. The grid (mesh) defines the geometry of the problem

under consideration as shown in Fig. 4. Medium size 15-node triangular element mesh is used to run the model within a reasonable time limit and yet yield higher accuracy. Ground water head or external water pressure is not taken into consideration.

Table 1: Laboratory rock mechanic parameters used in the numerical model

Parameters	Rock Type		
	Metabasics	**Slumped rockmass**	**Crushed rockfill along open joints**
Density	24 kN/m^3	18 kN/m^3	---
Uniaxial Compressive Strength (UCS)	41 MPa	---	---
Deformation Modulus	3 GPa	0.01 GPa	0.01 GPa
Poisson's ratio, ν	0.3	0.3	0.3
Cohesion, *c*	3 MPa	0.005 MPa	0.005 MPa
Friction Angle, φ	33º	20º	24º
Dilation angle	10º	0º	0º
Geological Strength Index (GSI)	50	---	---
m_i	10	---	---
Normal Stiffness, k_n	---	---	1 GPa
Shear Stiffness, k_s	---	---	0.1GPa
Mode of Failure	Hoek-Brown	Mohr-Coulomb	Mohr-Coulomb

Strength reduction technique was applied in the model to reduce the strength parameters (i.e. friction angle and cohesive force) of rock mass during the computation process to make slope reach the failure condition. The strength reduction method is selected when it is desired to calculate global factor of safety (FoS) for a given situation. Therefore, $\varphi - c$ reduction process is also adopted for calculating FoS. The critical slope angle is the key factor in the slope failure analysis. The deformation of mesh shown in Fig. 4 is maximum at the toe as shown in Fig. 5, since the toe is under heavy strain and is always vulnerable in a steep and large slope. The displacement of the toe of the slope leads to the formation of a failure zone as shown in Fig. 6. The total displacement as calculated by the model is 0.15mm. The mode of failure of the slope is circular and critical depth of the failure zone is around 10m. FoS of the slope as calculated by the model is 1.99 after 120 iterations as shown in the graph in Fig.7. Fig. 8 shows the accumulation of maximum principal strain which commensurate with the depth of slip circle. The principal strain is concentrated more at the middle at the slope due to the presence of crushed rock filled valley dipping open joints of weak strength and forms a circular zone of failure.

A limit equilibrium (LEM) modelling with the help of Slide ver. 6.0 software was carried out to correlate with the FoS value determined from the FEM using the same parameters for metabasics, slumped rockmass and crushed rock fill open joints. The deterministic factor of safety and critical slip circles are shown in Fig. 9. The FoS value was determined using Bishop simplified (BS) limit equilibrium method. The advantage of using BS method is that it considers the interslice normal forces and the equation for FoS hence become non-linear. However, it neglects the interslice shear forces. FoS is calculated for circular shear surface using the following equation:

$$F_m = \frac{\sum(c'l + N'tan\varphi')}{\sum W\ sin\alpha} \quad (1)$$

where F_m= FoS for Moment equilibrium, c' = effective cohesion, N'=effective base normal force, φ'= effective internal angle of friction, $\sum W\ sin\alpha$ = sum of driving forces

Effective base normal force, N' is given by the equation

$$N' = \frac{1}{m_\alpha}\sum\left(W - \frac{c'lsin\alpha}{F} - ulcos\alpha\right) \quad (2)$$

where, u=pore pressure, l=slice base length, α=inclination of slip surface at the middle of slice

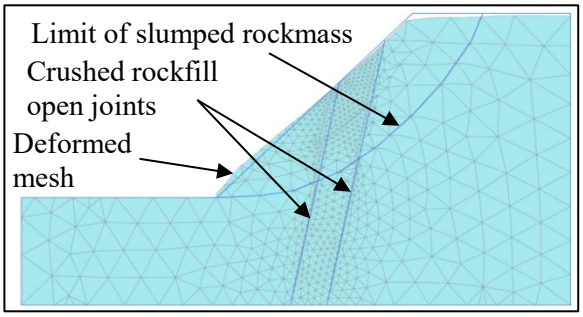

Fig. 4: Mesh generation showing deformed mesh

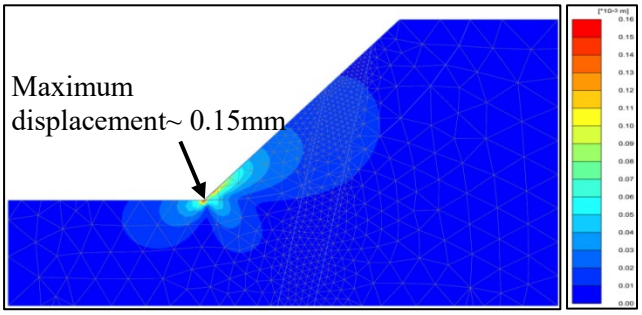

Fig. 5: Total displacement maximum at the toe of the slope

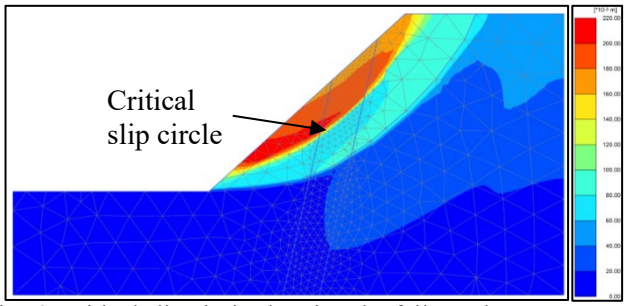

Fig. 6: Critical slip circle showing the failure plane

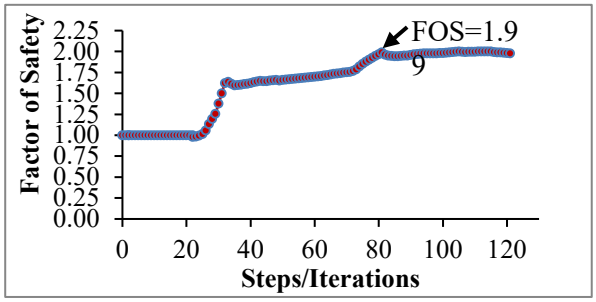

Fig. 7: Calculated FOS by the model after 120 iterations

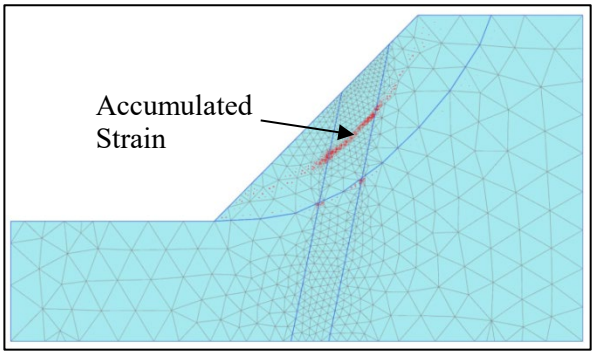

Fig. 8: Maximum principal strain accumulated at the middle of slope due to valley dipping joints of low shear strength.

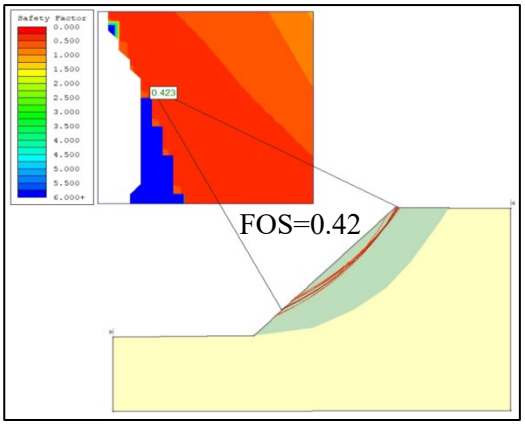

Fig. 9: Critical slip circle and calculated FOS determined by Slide

$$m_\alpha = cos\alpha \left(1 + tan\alpha \frac{tan\varphi'}{F}\right) \quad (3)$$

where m_α = moment equilibrium , F=FoS for Force equilibrium

Comparison of FoS values determined from FEM and LEM shows that both the models indicate development of critical slip circle of failure at a depth of 10-15m as shown in Fig. 6 and Fig. 9. Calculated FoS values from FEM is 1.99 as shown in Fig. 7 which indicates fairly stable condition. However, the same slope stability analysis in LEM calculates FoS values of 0.423 which indicates unstable slope condition. This difference in values can be interpreted by the fact that, FEM consider elastic parameters such as Young's modulus and Poisson's ratio in their material properties and lay more emphasis on the geometry of the slope whereas LEM considers uniaxial compressive strength of the rock, disturbance factors like blasting damage during slope excavation and also m_i and s parameters of Hoek-Brown. Thus based on the experience of sliding and slope failure experienced during excavation of powerhouse backslope, LEM appears to give a more realistic assessment of the instability of the powerhouse backslope than FEM.

3.6. Analysis of the Support Installed to Stabilize the Backslope

Redesign of powerhouse backslope excavation was carried out following its major failure. The excavation of the backslope started from EL ±1510M. A cross drain was constructed at El±1520M to drain out the surface runoff. The was cut down to the level of ±1330M. Thus a vertical slope of about 180m height with intermediate benches at 15m interval was to be stabilized, which was a challenging task.

Back analysis was carried out with the cable anchor support in the backslope of the powerhouse by LEM and the result shows that FoS increased considerably upto 1.7 as shown in Fig. 10. Thus installation of cable anchors restricted the movement of the slumped rockmass leading to the stabilization of rockmass which was also confirmed by various instrumentation readings installed in the powerhouse backslope. In addition, four number of drifts were excavated to carry out grouting of the open joints as shown in Fig. 2(b). The drifts were reinforced with steel and concrete up to crown to bear the induced stresses imparted by the rock cover.

As per the support analysis, cable anchors of length 35m were provided in the cutslope above each benches as shown in Fig. 11. The fixed and free length of the cable anchors are 9m and 26m respectively. The fixed 9m length at the end of cable anchor was fully grouted in the beginning and stressing was done for checking the performance of grout/fixed length.

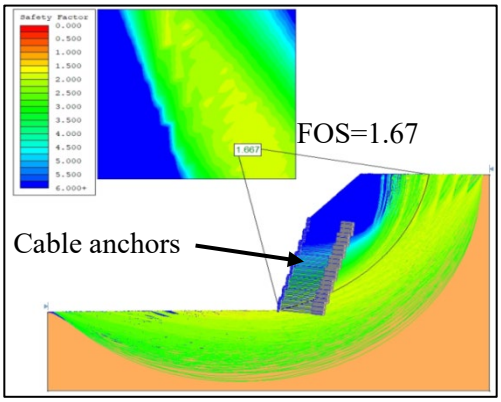

Fig. 10: LEM analysis showing increase in FoS value after installation of cable anchors .

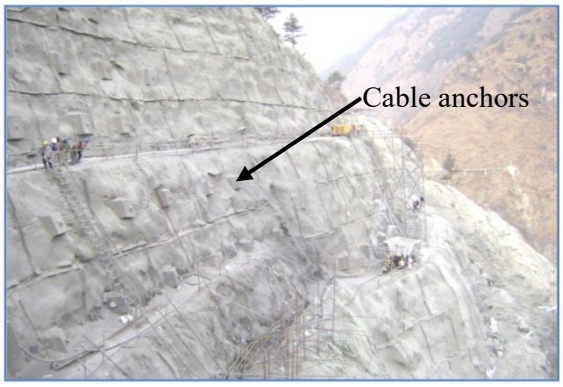

Fig. 11: Backslope stabilization by cable anchors

4. Back Analysis of Stress and Deformation Encountered during Rock Bursting

Based on the world stress map (2016), it is found that in the study area, the direction of in-situ vertical and horizontal stresses (S65°W) are oriented subparallel to the major joint set (270°/70°) and at high angle (50º) with the tunnel alignment (N195º) as shown in Fig. 12(a). According to Laubscher (1990), both the above conditions are conducive for rock bursting which has been experienced frequently during tunnel excavation in massive and brittle quartzite under a high superincumbent cover ranging from 750m to 1600m. On the basis of rock bursting events experienced during excavation in quartzite rockmass in head race tunnel (HRT) of Parbati hydroelectric project-II as shown in Fig.12 (b), back analysis of magnitude of in-situ stresses in rock bursting zones was carried out using FEM (Phase 2, v.8.0) to determine the role of strength, elastic properties of the rockmass and field stress ratio in causing rock bursting. Principal stress, deformation values and strength factor at two different stress ratios corresponding to minimum and maximum overburden cover of 750m and 1600m respectively were determined using numerical method.

In-situ vertical stress σ_V was calculated from the equation

$$\sigma_V = \gamma.Z \tag{4}$$

where γ = density of the rock, Z= superincumbent cover above the tunnel section

In-situ horizontal stress σ_H was calculated from Hoek and Brown (1980) equation:

$$K_0 = 0.4 + \frac{800}{Z} \tag{5}$$

where K_0 is the field stress ratio defined by the equation

$$K_0 = \frac{\sigma_H}{\sigma_V} \quad (6)$$

In this study, the rockmass inside the tunnel has been considered homogeneous, perfectly plastic material subjected to uniform near field stresses. Generalized Hoek and Brown failure criterion was adopted for calculation of stress and deformation parameters. Geotechnical parameters of the rockmass considered for study is shown in Table 2. From Fig. 13 (a & b), it can be interpreted that with decrease in field stress ratio, K_0 or with increase in in-situ stresses, σ_V and σ_H due to increase in depth of overburden, the values of principal stress, σ_1 and deformation, ε increase leading to the decrease in strength factor, S_f (<1.5) in both the crown and springline area of the tunnel. The yielding due to shear also concentrates more at lower field stress (K_0=0.97) while the yielding due to tension concentrates more in the area of intersection of the strike of the major joints with the tunnel axis (Fig.13 a, b).

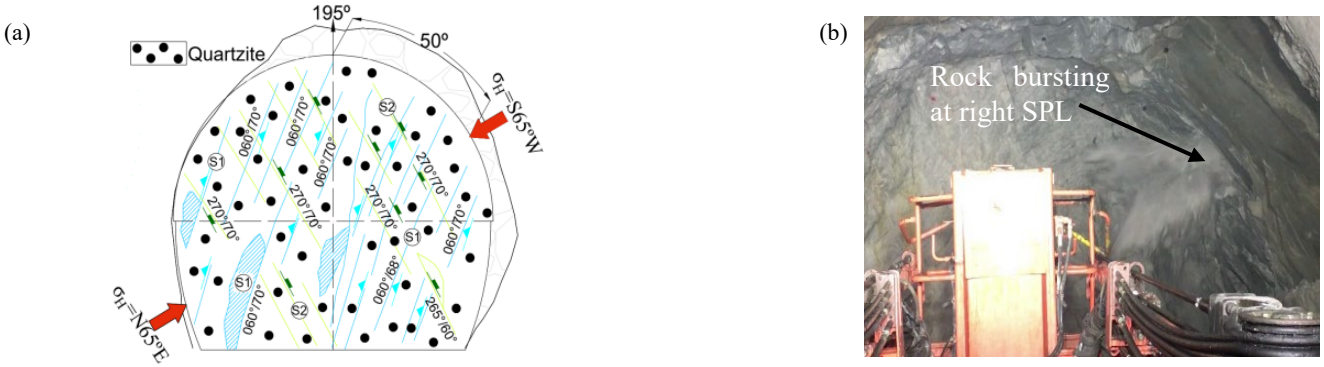

Fig. 12: (a) Geological face log of HRT showing principal stress directions (b) Rock bursting in right springline (SPL) area of HRT

Table 2: Geomechanical parameters of rockmass considered for the study

Rock type	Geomechanical parameters of rockmass									Stresses		
	Z (M)	GSI	UCS (MPa)	γ (MN/m^3)	m_i	φ (°)	*c* (MPa)	ν	E_i (GPa)			
Quartzite	750	70	100	0.026	20	48.5	31	0.2	41	1.47	20	29
	1600	70	100	0.026	20	48.5	31	0.2	41	0.9	42	37

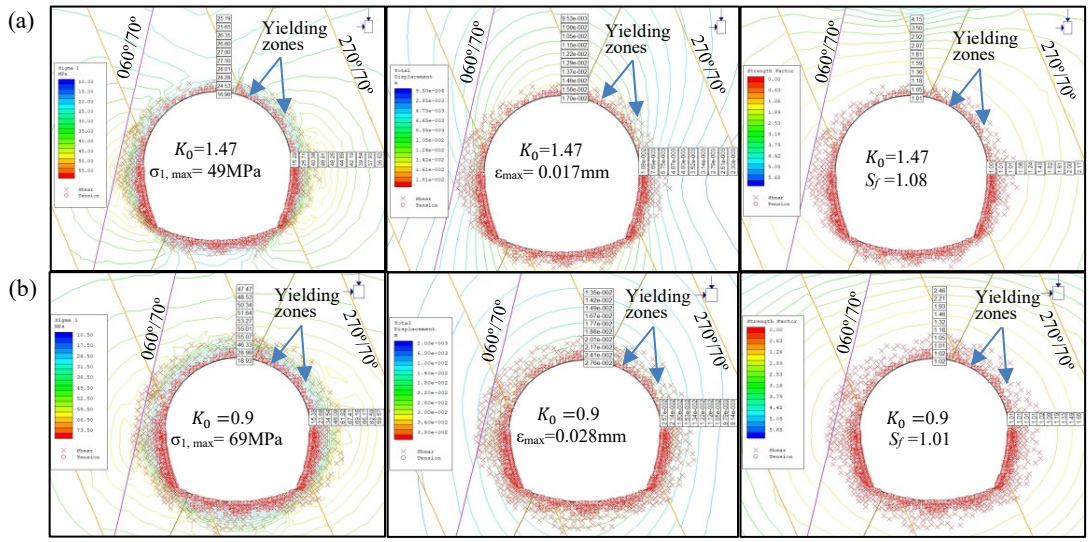

Fig. 13: Stress contours showing Principal stress (σ_1), displacement (ε) and strength factor (S_f) values at crown for two different stress ratios (a) K_0=1.47, (b) K_0=0.9 in study area

5. Conclusion

The paper reviews two events of geological hazards encountered in a mega hydropower project located in Lesser Himalayan region of India. The inferences drawn from the study are as follows:

(a) The factors causing major event of powerhouse backslope failure in the study area during construction and remedial measures adopted are discussed. Main geological factors leading to the failure are slumped rockmass of weak strength extending throughout the height of the slope, valley dipping open joints and crushed rock fill shear seams. Heavy rainfall further weakened the shear strength parameters of the rockmass and triggered failure.

(b) Stability analysis of the natural slope was carried out before excavation by Finite element numerical modelling and it was found that rockmass shows elasto-plastic deformation to the amount of 0.15mm in the toe area of the slope leading to the development of critical slip circle upto a depth of 10-15m. FoS calculated through LEM shows a value of 0.423 which is substantially lower than the desired factor of safety making the slope vulnerable to failure.

(c) After the failure, design of powerhouse was reviewed and to remove the slumped rock and locate the powerhouse backslope in sound rockmass, the height of the cutslope was further increased upto 180m with intermediate berms. As a result, the steepness of the slope also increased from 45º to 70º. Support analysis of the proposed cutslope was carried out through LEM and installation of fully grouted cable anchors of length more than 35m at a spacing of 2m c/c was found to be the most suitable support measure to stabilize the cut slope. Model shows considerable increase in FoS of the slope upto 1.7 after installation of cable anchors.

(d) Accordingly, support measures in the form of 35m long cable anchors, shotcrete, grouting through drifts alongwith concreting of the drifts to increase load bearing capacity were carried out for stabilization of the powerhouse backslope.

(e) For long term monitoring, instrumentation in the form of Multi-point borehole extensometer, Inclinometer and Load Cell were installed as shown in Fig. 2(b). No abrupt rise in the instrumentation reading was observed thus indicating that the powerhouse cut slope is stable with no appreciable movement or deformation.

(f) The reason for frequent rock bursting during tunnelling may be accounted due to unfavourable orientation of tunnel and major discontinuities intersecting the encountered rockmass w.r.t. the direction of principal stress. Stress analysis through numerical modelling shows that both yielding and deformation increase with decrease in field stress ratio i.e. with increase in overburden depth. Drilling of stress relief holes, installation of untensioned rock anchors at close spacing alongwith steel fibre reinforced shotcrete at crown and springline area of the tunnel were the remedial measures applied to tackle rock bursting.

Overall, the paper outlined major surface and subsurface geotechnical problems encountered during construction of a mega hydropower project in unfavourable geological conditions and remedial measures adopted to successfully negotiate the problems. The experience gathered is well documented and may act as an impetus for future study.

6. References

[1] K.S. Valdiya and S.K. Bartarya, “Diminishing discharges of mountain spring in a part of Kumaun Himalaya.” Current Sc., 1989, vol. 58, pp.417-426.

[2] S. Bhatnagar and R. Das, “Managing Powerhouse Back slope: A case study,” *Proceedings of* Indorock conference, India, 2013, pp. 575-583.

[3] T.N. Singh, V. Bhardwaj, L. Dhonta and K. Sarkar, “Numerical analysis of instability of slope near Rudraprayag area, Uttaranchal, India,” Jour. Engg. Geol, 2005, vol. 34, pp. 33-41.

[4] D.H. Laubscher, “A geomechanics classification system for the rating of rockmass in mine design,” J S Afr Inst Min Metall, 1990, vol.90, pp. 257-273.

[5] World Stress Map,“World stress map based on the database release 2016,” http://www-wsm.physik.uni-karlsruhe.de/pub/stress_data/stress_data_frame.html, 2016.

[6] E. Hoek and E. T. Brown, “Underground excavations in Rock,” The Institute of Mining and Metallurgy, London, 1980.